PERGAMON

International Journal of Solids and Structures 39 (2002) 1327–1335

INTERNATIONAL JOURNAL OF SOLIDS and STRUCTURES

www.elsevier.com/locate/ijsolstr

A generalised stress intensity approach to characterising the process zone in complete fretting contacts

A. Mugadu [1], D.A. Hills *

Department of Engineering Science, Lincoln College, Oxford University, Parks Road, Oxford, OX1 3PJ, UK

Received 13 January 2001; received in revised form 17 August 2001

Abstract

The known analytical contact solution for the stress field induced by a rigid, square-ended punch, sliding on an elastic half-plane defines the stress state everywhere in the half-plane. An asymptotic approach is then used to determine the characteristic stress field at the edge of the contact, which is matched with the contact solution. Hence, the regions over which the asymptotic solution is valid are found. Using a method analogous to the crack-tip stress field, a generalised stress intensity factor is defined, with the aim of providing a single variable characterisation of the stress state at the punch corner. The crack initiation process zone for a fretting fatigue crack is therefore captured, and the conditions for small scale yielding explicitly found.

Keywords: Fretting fatigue; Complete contacts; Asymptotic solution

1. Introduction

Fretting fatigue occurs much more frequently in components under 'complete contact' conditions, than it does between incomplete contacts. Examples include spline joints between shafts, most kinds of bolted connections, and certain geometries of gas turbine fanblade dovetails. These contacts pose a different problem from those between incomplete contacts because it is impossible, even in principle, to specify directly how initiation conditions depend on the contact tractions, simply because they must always assume an infinite value, implied by an elasticity solution, at the edge of the contact. One possible approach is to use critical plane methods, and to circumvent the local stress infinity by stating that the critical parameter must be present over a particular finite volume. The main argument in favour of this is that the quantity which causes initiation must be sufficiently widespread to cause the embryo crack to propagate into adjacent grains, when the transition towards a propagation type of crack growth could be said to take over. Although this is certainly a feasible approach, and has been used in practice (Araújo and Nowell, 2000), there are alternatives.

* Corresponding author. Fax: +44-01865-273-813.
E-mail address: david.hills@eng.ox.ac.uk (D.A. Hills).
[1] Sponsored by the Rhodes Trust, DPhil. Research Student.

0020-7683/02/$ - see front matter
PII: S0020-7683(01)00210-4

Here, we intend to use the asymptotic stress field adjacent to the corner of the contact as a unique means of characterising the environment in which the crack nucleates. The asymptotics of the stress field adjacent to a locally slipping pad-corner have recently been studied in some detail Mugadu et al., in press. This approach will here be applied to the problem of a rigid, square-ended punch, pressed into an elastic half-plane of finite stiffness, and subject to a shearing force sufficient to cause sliding. This could realistically be attained under displacement-controlled conditions. We will go on to examine the complete contact stress field, and to deduce the generalised stress intensity factor associated with the asymptotic solution. From there, the spatial variation of the stress field given by the asymptotics will be found, and compared with the full field solution, in order to find the extent over which it dominates the solution. Hence, the maximum load will be found for the process zone to be completely controlled by the dominant singular term, i.e. the conditions under which small scale yielding applies will be found. Lastly, the application of the method to problems of designing against fretting fatigue will be discussed.

2. Sliding contact problem

The problem of a rigid, square-ended punch, of half-width a, sliding on an elastic half-plane, Fig. 1(a), may be solved in closed form. As the punch is rigid, we are concerned only with the deformation of the half-plane, and the surface normal displacement, $v(x)$, is related to the direct and shear tractions, $p(x)$ and $q(x)$ respectively, by Hills et al. (1993)

$$\frac{\partial v}{\partial x} = -\frac{\kappa+1}{4\pi\mu}\int_{-a}^{a}\frac{p(\xi)\mathrm{d}\xi}{x-\xi} - \frac{\kappa-1}{4\mu}q(x), \tag{1}$$

where κ is Kolosov's constant ($= 3 - 4\nu$ in plane strain, where ν is Poisson's ratio), and μ is the modulus of rigidity. If the punch is sliding, the tractions are everywhere related by

$$q(x) = -fp(x), \tag{2}$$

where f is the coefficient of friction. Note that in Eq. (2) above, $p(x) < 0$ (contact pressure), and additionally, f will be permitted to be of either sign. Positive values will denote sliding to the right (in the positive x-direction), thereby generating positive shear tractions on the half-plane (Fig. 1(a)), and negative

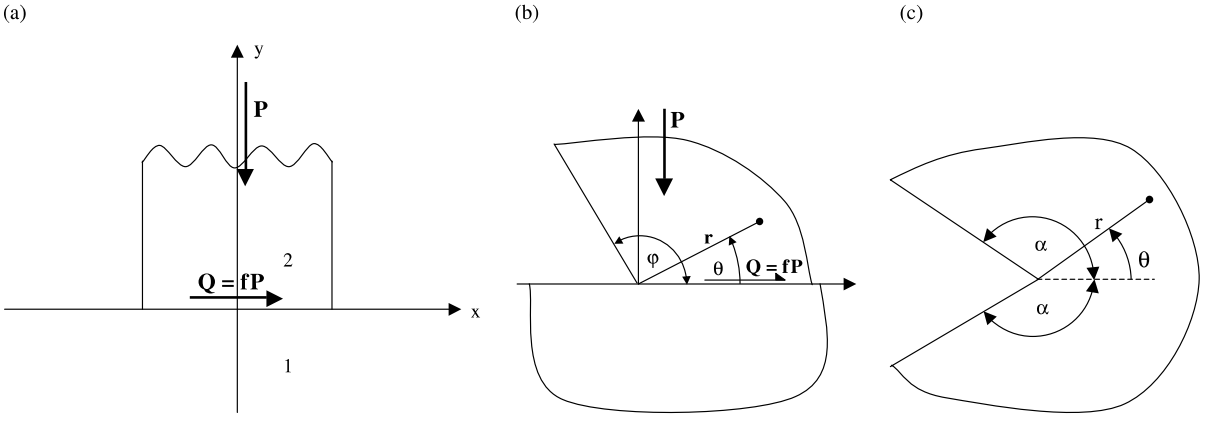

Fig. 1. (a) Representation of a square-ended rigid punch on an elastic half-plane, (b) a wedge sliding on an elastic half-plane, (c) a notch of internal angle 2α.

values sliding to the left, hence giving negative shear tractions. The reasons behind this convention will become clearer in the next section.

The surface normal displacement, $v(x)$, is constant in the range $-a \leqslant x \leqslant +a$ and hence Eq. (1) becomes

$$0 = \frac{1}{\pi} \int_{-a}^{a} \frac{p(\xi)\mathrm{d}\xi}{x - \xi} + f\beta p(x) \tag{3}$$

which is a standard Cauchy singular integral equation of the second kind, and Dundurs' constant, β, takes on a simplified form as one body is rigid, viz.

$$\beta = \frac{1 - 2v}{2(1 - v)}. \tag{4}$$

This may be inverted by the well-known Riemann–Hilbert procedure Hills et al. (1993), Muskhelishvili (1953) and, when a singular-both-ends solution is sought, yields

$$\frac{p(x)a}{P} = -\frac{\sin \lambda\pi}{\pi}(1 - x/a)^{\lambda-1}(1 + x/a)^{-\lambda}, \tag{5}$$

where

$$\tan \lambda\pi = \frac{1}{f\beta} = \frac{2(1 - v)}{f(1 - 2v)} \quad 0 < \lambda < 1. \tag{6}$$

Fig. 2 shows a plot of the variation of λ with f and β. Dundurs' parameter, β, varies such that $0 \leqslant \beta \leqslant 0.5$ which, from Eq. (4) above, corresponds to $0.5 \geqslant v \geqslant 0$. Here we see that the order of singularity is stronger at $x = -a$, when the shear tractions are negative $(-f)$ and weaker when positive $(+f)$. Conversely, at $x = +a$, a negative value of f leads to a weaker singularity, and a positive value of f to a stronger singularity.

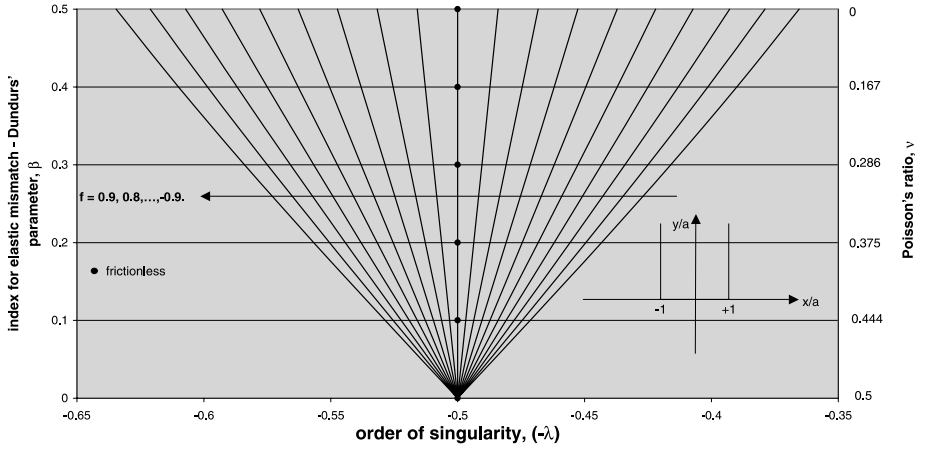

Fig. 2. Plot of β and v, against the order of singularity $(-\lambda)$ for a rigid square-ended punch on an elastic half-plane for different coefficients of fricition, f, at $x/a = -1$.

3. Asymptotic solution

Asymptotic analyses of problems in elasticity theory were pioneered by Williams (1952), who developed solutions for the state of stress near a sharp apex in a body under various boundary conditions. The theory was subsequently applied to the problem of a sliding contact along a frictional interface (Fig. 1(b)) between a wedge and an elastically dissimilar half-plane by Gdoutos and Theocaris (1975) and Comninou (1976). Details of the underlying analysis can be found in Bogy (1971), and here, only the salient points will be noted. The eigenvalues, λ_1, correspond to the smallest roots of the characteristic equation

$$D = (1+\alpha)\cos\pi\lambda_1(\sin^2\varphi\lambda_1 - \lambda_1^2\sin^2\varphi) + \tfrac{1}{2}(1-\alpha)\sin\pi\lambda_1(\sin 2\varphi\lambda_1 + \lambda_1\sin 2\varphi) + f\sin\pi\lambda_1\left[(1-\alpha)\lambda_1(1+\lambda_1)\sin^2\varphi - 2\beta(\sin^2\varphi\lambda_1 - \lambda_1^2\sin^2\varphi)\right] = 0. \tag{7}$$

Clearly, λ_1 is a function of $(f, \varphi, \alpha, \beta)$, where α represents Dundurs' first parameter (here, unity because the wedge is rigid) and φ, the internal angle of the wedge (here $\pi/2$) (Fig. 1(b)). The order of singularity in the stresses near the apex of the wedge is then given by

$$\sigma_{ij} = 0(r^{\lambda_1 - 1}) \quad \text{as } r \to 0 \quad \text{for } \lambda_1 \text{ real and } 0 < \lambda_1 < 1, \tag{8}$$

where r is a polar coordinate measured from the wedge corner (Fig. 1(b)).

Turning to the contact problem, we note that the stress state near the punch corners may be seen from Eq. (5) to vary in the form

$$\sigma_{ij} = \left\{ \begin{matrix} 0(r^{\lambda-1}) & \text{at } x = a \\ 0(r^{-\lambda}) & \text{at } x = -a \end{matrix} \right\} \quad \text{as } r \to 0. \tag{9}$$

As noted earlier, the order of singularity differs at each punch-corner depending on the direction of applied shear. We also noted that when looking at the left hand corner $(x = -a)$, the singularity is greater for negative f and less for positive f. This behaviour is consistent with that observed in the asymptotic problem given above and hence, without loss of generality, we shall focus our attention here. The exponents in Eq. (8) and the second of Eq. (9) are then equal leading to the relationship $\lambda + \lambda_1 = 1$.

Lastly, the presence of different orders of singularity with different senses of the shear force complicates the characterisation of the process zone, and this will be discussed later.

3.1. Application to contact problem

The form of the local stress state at the corner of the punch has been found. In order to determine its extent we need to match the asymptotic solution to the full field solution. The best way to do this is to employ procedures based on fracture mechanics principles. For a crack, we note that the mode I stress intensity factor, K_I, may be defined as

$$K_I = \lim_{r\to 0}\sqrt{2\pi r}\sigma_{yy}(r), \tag{10}$$

where r is the distance ahead of the crack-tip and σ_{yy} is the stress component perpendicular to the crack axis. By analogy, we define a generalised stress intensity factor, K^*, by

$$K^* = \lim_{r\to 0} p(r)r^{\lambda}. \tag{11}$$

This may be applied to the contact problem by making the substitution $r = x + a$, and taking the limit $x \to -a$, i.e. for the left hand corner of the punch (Fig. 1(a)). Applying this procedure to Eq. (5) leads to the following solution for the normalised generalised stress intensity factor

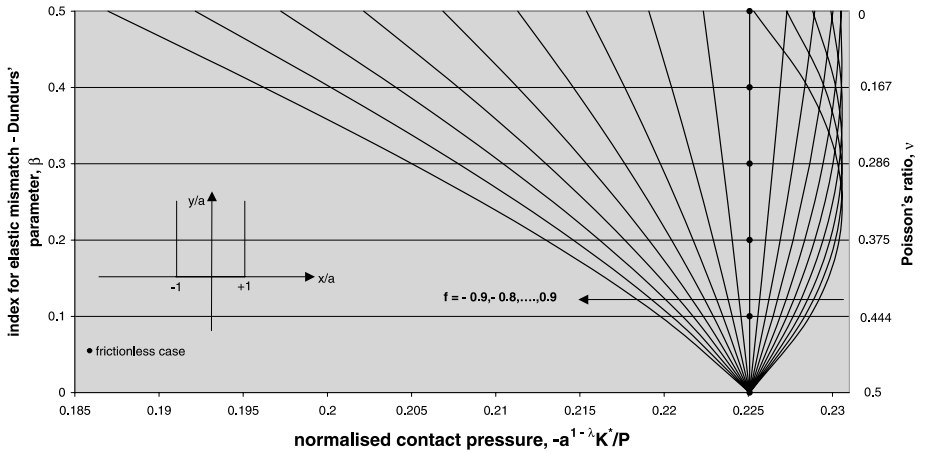

Fig. 3. Plot of the β and v against the normalised contact pressure, $-a^{1-\lambda}K^*/P$, for a rigid square-ended punch on an elastic half-plane for different coefficients of friction, f, at $x/a = -1$.

$$\frac{a^{1-\lambda}K^*}{P} = -\frac{\sin\lambda\pi}{\pi 2^{1-\lambda}}, \tag{12}$$

and the variation of this quantity with f and β is shown in Fig. 3.

3.2. Small scale yielding

The motivation behind this analysis is to provide a single parameter characterisation of the process zone at the punch-corner, where cracks nucleate. The object is to pursue an analogy with fracture mechanics, in which crack development is controlled by the crack-tip singular field, characterised by the crack-tip stress intensity factor. In order for this procedure to hold, the process zone must be contained wholly within a region in which the singular term dominates the stress field. In fact, it must be rather smaller than the extent of the singular term dominated region, in order for the effect of the plastic region on the singular field itself to be negligible. Just as in fracture mechanics where we may compare the full Westergaard solution with the Irwin–Kolosov singular solution (McKellar et al., 2000), here the asymptotic solution may be compared with the exact internal contact stress state within the half-plane. The Muskhelishvili potential corresponding to the traction distribution found is given by Hills et al. (1993)

$$\Phi(z) = (\mathrm{i}+f)\frac{P}{2a\pi}\frac{\operatorname{cosec}\lambda\pi}{(z-1)^{1-\lambda}(z+1)^{\lambda}}, \tag{13}$$

where $z = x + \mathrm{i}y$, and $\mathrm{i} = \sqrt{-1}$. When once the potential is known, the interior stress field may easily be found from standard results, by differentiation alone.

Turning to the asymptotic stress field, we may find its spatial variation by determining the eigenvector corresponding to a particular eigenvalue. The eigenfunctions may then be deduced by back substituting these coefficients. This then fully specifies the variation of the stress components with (r,θ), with the multiplicative constant given by the generalised stress intensity factor.

Fig. 4(a) and (b) displays the individual components of stress implied by the singular solution and in Fig. 5, we show the second invariant of the stress deviatoric tensor, representing the von-Mises' yield parameter,

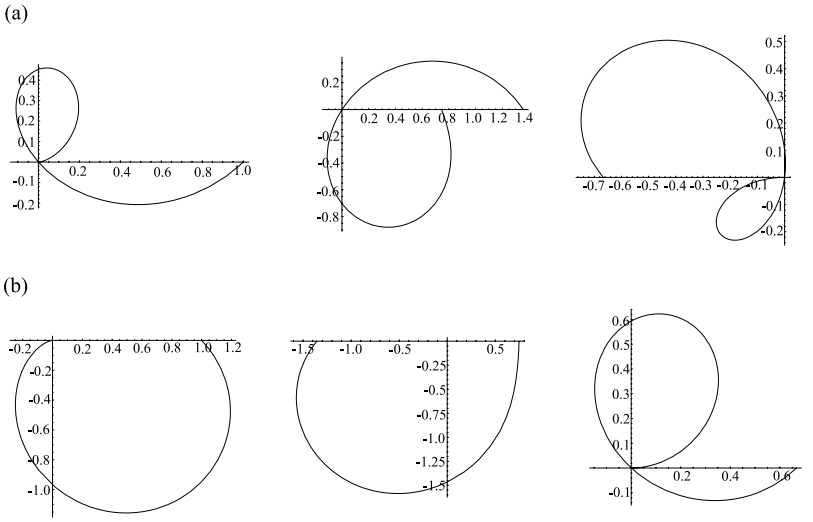

Fig. 4. Polar plots of stress components, $\sigma_{\theta\theta}r^{1-\lambda_1}/K^*$, $\sigma_{r\theta}r^{1-\lambda_1}/K^*$ and $\sigma_{rr}r^{1-\lambda_1}/K^*$ for (a) $f = 2/3$ and (b) $f = -2/3$.

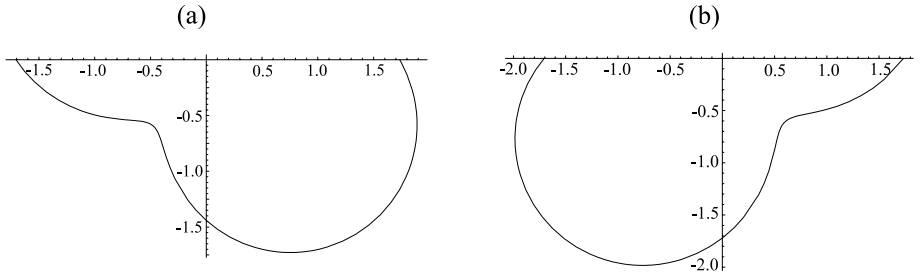

Fig. 5. Polar plots of the von-Mises' yield parameter, $r^{1-\lambda_1}\sqrt{J_2}/K^*$ for (a) $f = 2/3$ and (b) $f = -2/3$.

and hence the general form of the shape of the process zone. The representative values of the variables used in this analysis were $f = \pm 2/3$ and $v = 0.3$.

Clearly, the full contact stress field and the asymptotic field differ at any finite distance from the punch-corner, and this is displayed in Fig. 6(a) and (b), which characterise the stress field by the von-Mises' yield parameter. The quantity plotted is a set of contours of $\left[\left(\sqrt{J_2}_{\text{full}} - \sqrt{J_2}_{\text{asymp}}\right)/\sqrt{J_2}_{\text{full}}\right]$ as a function of position, and hence this represents the fractional error in using the singular field to characterise the true near-corner stress field. Fig. 6(a) applies when the shear force is directed *away* from the corner ($f = 2/3$), and Fig. 6(b) applies when the shear force is directed *towards* the corner ($f = -2/3$). These plots may be used in conjunction with Fig. 7(a) and (b) respectively, which show the *extent* of the plastic field implied by the elastic contact stress field. The contours are labelled in terms of P/ak, where k is the yield stress of the material in pure shear, and this quantity therefore represents the dimensionless ratio of the mean contact pressure to the yield stress: for a given value of this normalised contact load, the extent of the yield zone (not, of course, allowing for any stress redistribution associated with plastic flow) is given by the relevant contour in Fig. 7. If this is then compared with the magnitude of the maximum contour in Fig. 6 which spatially intersects the yield front, a good estimate of the accuracy of the solution will be found, and hence a judgement may be made on the validity of the assumption of small scale yielding.

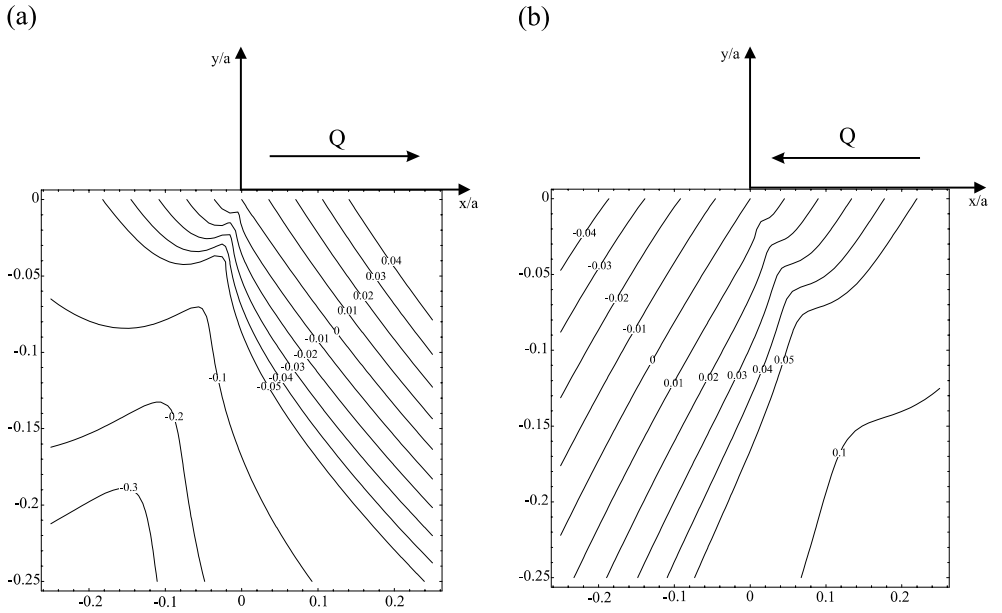

Fig. 6. (a) Plot of $(\sqrt{J_{2\text{full}}} - \sqrt{J_{2\text{asymp}}})/\sqrt{J_{2\text{full}}}$ for $f = 2/3$. (b) Plot of $(\sqrt{J_{2\text{full}}} - \sqrt{J_{2\text{asymp}}})/\sqrt{J_{2\text{full}}}$ for $f = -2/3$.

3.3. Influence of next term in expansion

In the above analysis, attention was focused on identifying the first term in the asymptotic expansion, the so-called dominant singular term. In any real problem, there may be a second singular term which would

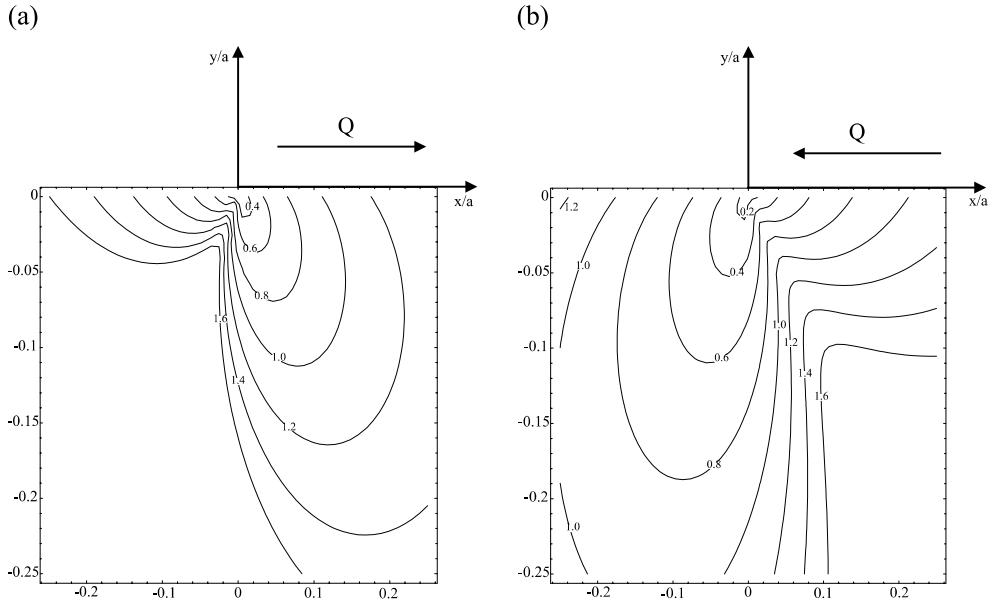

Fig. 7. (a) Plot of the normalised punch load, P/ak for $f = 2/3$.

have an influence on the state of stress at the edge of the contact. This leads to the question of how significant the stress state associated with the second term might be, and hence throw into doubt the accuracy of a solution based on the dominant singular term alone. For a sliding contact, determining the next term would require extensive further analysis, but a useful indicator is to consider the Williams' solution (Williams, 1952)—the "adhered" form of the contact.

Owing to the nature of the geometry of the Williams' solution, the strongest and second strongest eigenvalues ($\lambda_{\min}$ and $\lambda_{\min+1}$) correspond to symmetric and anti-symmetric loading (Barber, 1992). If we let 2α represent the internal notch angle (Fig. 1(c)) then for small angles i.e. slightly greater than 180°, we see from Barber (1992) that, the eigenvalues representing the two types of loading are widely separated, but they become closer as 2α increases, converging to 0.5 as $2\alpha \to 360°$. A further complication which arises is that the multiplicative constants for the two solutions (the generalised stress intensity factors) may make the relative contributions from the two terms closer or further apart, depending on their relative values: thus if the mode II generalised stress intensity factor (for anti-symmetric loading) is much greater than that for mode I, the relative contributions would be pushed closer together, and it would not be acceptable to use a dominant term only solution.

We turn, now, to an application of these considerations to the punch/half-plane problem. For this restricted calculation, the contact is assumed to be adhesive, and the half-plane incompressible. Now, $2\alpha = 270°$, giving $\lambda_{\min} = 0.544484$ (symmetric) and $\lambda_{\min+1} = 0.908529$ (anti-symmetric). The stress state implied by these eigenvalues varies as $r^{\lambda_2 - 1}$, where λ_2 represents the eigenvalue to the problem and r is a polar coordinate measured from the apex of the notch (Fig. 1(c)). We then obtain the spatial variation of stress around the 'notch' and hence, expressions for the generalised stress intensity factors may be defined as

$$\sigma_{\theta\theta} r^{1-\lambda_{\min}} = K_1^* \quad \text{symmetrical loading,} \tag{14}$$

and

$$\sigma_{r\theta} r^{1-\lambda_{\min+1}} = K_{11}^* \quad \text{anti-symmetrical loading} \tag{15}$$

at $\theta = 0$, where θ is measured from the line bisecting the internal angle. For the case being considered, $K_1^* = 2.389$ and $K_{11}^* = 2.114$. These results show that the multipliers are comparable in magnitude and so, as the exponents for the two terms are quite widely separated, the term with the stronger singularity, i.e. symmetrical loading, will dominate the problem, and the assumption made is justified.

4. Conclusion

The paper has described the development of an asymptotic approach to the characterisation of the stress field present near the corner of a sharp punch, under slipping frictional contact conditions. The punch-corner field has then been displayed in different forms, so as to show the implied process zone size and shape, where cracks nucleate under fretting conditions. This gives the possibility of using a fretting fatigue experiment with simplified geometry (Limmer et al., 2001) to represent the crack initiation conditions in prototypes of complex shape, but where contact is complete. In order to represent the nucleation environment with good fidelity it is necessary to represent the process zone precisely, and this may be done by matching the generalised stress intensity factor, and slip displacement. Most problems will require the numerical solution of the contact problem by finite elements, but this particular problem affords a closed form solution, which may be used as a benchmark calibration, and illuminates other aspects of the problem such as the limitations of small scale yielding, which are very time consuming to probe numerically.

One aspect of the problem which merits comment is that, when the punch suffers a reversing shearing force, each corner of the punch sees, alternately, a shearing stress directed towards, and then away from the

corner, as shown by the results for $\pm f$ in Fig. 2. This means that, quite aside from questions of plastic shakedown and the self-development of residual stress fields at the punch-corners, there will be two implied asymptotic elastic stress states present alternately, one of a higher strength singularity than the other. The relative magnitudes of the stress states corresponding to these two halves of the loading cycle can be judged partly from the order of the singularity present in each half cycle, and partly from the relative magnitudes of the generalised stress intensity factors. In any particular problem, the relative importance of each half of the cycle may be judged by noting the extent of the process zone for each half of the cycle. Where they are comparable in magnitude, the effects of each will need to be identified separately.

Lastly, the issue of the "next term" in the asymptotic expansion has been briefly addressed using the Williams' solution. Although this has not been tackled for a sliding contact, the results suggest that using the dominant singular term represents a relatively accurate means of characterising the stress state at the edge of a sliding, square-ended rigid contact.

Acknowledgement

The authors would like to thank the referees for their constructive criticism.

References

Araújo, J.A., Nowell, D., 2000. Prediction of fretting fatigue life using volume averaged multiaxial initiation parameters. In: Becker, A.A. (Ed.), EMAS, Proceedings of the fourth International Conference on Modern Practices in Stress and Vibration Analysis, Nottingham, United Kingdom 5–7 September, pp. 223–234.

Mugadu, A., Hills, D.A., Limmer, L., 2001. An asymptotic approach to crack initiation in complete contacts. J. Mech. Phys. Solids 215, 105–112.

Hills, D.A., Nowell, D., Sackfield, A., 1993. Mechanics of Elastic Contacts. Butterworth Heinemann, Oxford.

Muskhelishvili, N.I., 1953. Some Basic Problems of the Mathematical Theory of Elasticity. Noordhoff, Gronigen.

Williams, M.L., 1952. Stress singularity from various boundary conditions in angular corners of plates in extension. J. Appl. Mech. 19, 526–528.

Gdoutos, E.E., Theocaris, P.S., 1975. Stress concentration at the apex of a plane indenter acting on an elastic half plane. J. Appl. Mech. 42, 688–692.

Comninou, M., 1976. Stress singularity at a sharp edge in contact problems with friction. J. Appl. Math. Phys. (ZAMP) 27, 493–499.

Bogy, D.B., 1971. Two edge-bonded elastic wedges of different materials and wedge angles under surface tractions. J. Appl. Mech. 38, 377.

McKellar, D.K., Hills, D.A., Nowell, D., 2000. A comparison between actual and stress intensity near-crack-tip elastic fields. Int. J. Fatigue 22, 551–558.

Barber, J.R., 1992. Elasticity. Kluwer, Dordrecht.

Limmer, L., Nowell, D., Hills, D.A., 2001. A combined testing and modelling approach to the prediction of fretting fatigue performance of splined shafts. Proc. I. Mech. E., Part G, J. Aero Engng., in press.